# Left Atrial 4-Dimensional Flow Magnetic Resonance Imaging
## *Stasis and Velocity Mapping in Patients With Atrial Fibrillation*

*Michael Markl, PhD,*† Daniel C. Lee, MD,*‡§ Jason Ng, PhD,‡§ Maria Carr, RT (MR),* James Carr, MD,* and Jeffrey J. Goldberger, MD‡§‖*

**Objectives:** Left atrial (LA) 4-dimensional flow magnetic resonance imaging (MRI) was used to derive anatomic maps of LA stasis, peak velocity, and time-to-peak (TTP) velocity in patients with atrial fibrillation (AF) and to identify relationships between LA flow with LA volume and patient characteristics.

**Materials and Methods:** Four-dimensional flow MRI for the in vivo assessment of time-resolved 3-dimensional LA blood flow velocities was performed in 111 subjects: 42 patients with a history of AF and in sinus rhythm (AF-sinus), 39 patients with persistent AF (AF-afib), 10 young healthy volunteers (HVs), and 20 age-appropriate controls (CTRL). Data analysis included the 3-dimensional segmentation of the LA and the calculation of LA stasis, peak velocity, and TTP maps. Regional LA flow dynamics were quantified by calculating mean stasis, peak velocity, and TTP in the LA center region and the region adjacent to the LA wall.

**Results:** A sensitivity analysis identified thresholds for global LA stasis (<0.1 m/s) and peak velocity (top 5% LA velocities), which detected significant differences between AF patients and controls for global LA stasis (HV, 25% ± 5%; CTRL, 29% ± 10%; AF-sinus, 41% ± 13%; AF-afib, 52% ± 17%) and peak velocity (HV, 0.43 ± 0.02 m/s; CTRL, 0.37 ± 0.04 m/s; AF-sinus, 0.33 ± 0.05 m/s; AF-afib, 0.30 ± 0.05 m/s). Regional analysis revealed significantly increased stasis at both LA center and wall for AF patients compared with age-appropriate controls (29%–84% difference, $P < 0.006$) and for AF-afib versus AF-sinus patients (22%–30% difference, $P < 0.004$). In addition, stasis close to the LA wall was significantly elevated ($P < 0.001$) compared with the LA center for all subject groups. Multiple regressions revealed significant ($R^2_{Adj} = 0.45$–$0.50$, $P < 0.001$) relationships between impaired global LA flow (reduced velocity and increased stasis) with age ($|\beta| = 0.27$–$0.50$, $P < 0.002$) and LA volume ($|\beta| = 0.26$–$0.50$, $P < 0.003$).

**Conclusions:** Atrial 4-dimensional flow MRI detected changes in global and regional LA flow dynamics associated with AF, age, and LA volume. Longitudinal studies are needed to test the diagnostic value of LA flow metrics as potential risk factors for thromboembolic events.

**Key Words:** atrial fibrillation, 4D flow MRI, left atrium, stasis, peak velocity, stroke

(*Invest Radiol* 2016;00: 00–00)

Atrial fibrillation (AF) is the most common cardiac arrhythmia, affecting approximately 33.5 million patients worldwide.[1] The most serious complication from AF is stroke, which is attributed to embolism of thrombus from the left atrium (LA).[2] Studies utilizing transesophageal echocardiography (TEE) have shown that impaired flow in the LA is an independent risk factor for thrombus formation and stroke in AF.[3–5] Furthermore, presence of spontaneous echo contrast, a marker of blood stasis, has been shown to predict thromboembolism.[3,6,7] Other TEE studies have shown that LA size and shape may be additional parameters influencing thromboembolic risk.[8–10] However, TEE requires esophageal intubation and the standard 2-dimensional (2D) imaging cannot fully assess the complex 3-dimensional (3D) pattern of flow and stasis in the LA.

Four-dimensional (4D) flow magnetic resonance imaging (MRI) can overcome these limitations by providing the ability to noninvasively measure complex 3D blood flow patterns in vivo.[11–13] A number of studies have demonstrated that 4D flow MRI is well suited for the comprehensive assessment of cardiac[14–17] and LA flow dynamics.[18–20] Moreover, it has recently been shown that 4D flow MRI can assess LA flow patterns in patients with AF.[21] However, previous studies did not provide an intuitive visualization and quantitative evaluation of LA flow and LA stasis. In addition, information on the choice of thresholds to detect differences in LA flow parameters and LA stasis between groups of AF patients and controls is lacking.

It was the aim of this study to test the potential of novel tools (anatomic maps of LA stasis, peak velocity, and TTP velocity) for the characterization of LA volume and flow, all derived from a single 4D flow MRI scan. We hypothesized that 4D flow-derived metrics of LA flow dynamics can detect differences between groups of AF patients and controls and identify relationships between global and regional LA flow, LA volume, and patient characteristics.

## METHODS

### Study Cohort

A total of 111 subjects were included in the study (81 patients with AF and 30 healthy controls). Atrial fibrillation patients included 42 subjects with a history of AF and in sinus rhythm during MRI (AF-sinus; age, 62 ± 11 years; 13 females) and 39 AF patients who were in AF at the time of imaging (AF-afib; age, 66 ± 11 years; 11 females). In addition, 10 young healthy volunteers (HVs; age, 24 ± 2 years; 4 females) and 20 age-appropriate controls (age, 59 ± 7 years; 7 females) were included. All subjects for this Health Insurance Portability and Accountability Act–compliant study were included in the study according to procedures approved by the Northwestern University institutional review board.

### Magnetic Resonance Imaging

All MRI examinations were performed on 1.5 T and 3 T MRI systems (Espree, Aera, Avanto, and Skyra; Siemens, Germany). All patients underwent standard-of-care cardiac MRI including retrospectively electrocardiogram (ECG)-gated time-resolved (CINE) balanced steady-state free precession imaging in 4-chamber, 2-chamber, and short-axis orientation of the left ventricle to evaluate left ventricular ejection fraction (LVEF). In addition, prospectively ECG-gated time-resolved 3D phase-contrast (PC) MRI with 3-directional velocity encoding (4D flow MRI) was employed to measure in vivo 3D blood flow velocities in the LA. Four-dimensional flow MRI data were acquired during free breathing using navigator gating of the diaphragm

Received for publication March 17, 2015; and accepted for publication, after revision, August 22, 2015.

From the *Department of Radiology, Feinberg School of Medicine, Northwestern University, Chicago; †Department of Biomedical Engineering, McCormick School of Engineering, Northwestern University, Evanston; ‡Division of Cardiology, §Feinberg Cardiovascular Research Institute, and ‖Center for Cardiovascular Innovation, Department of Medicine, Feinberg School of Medicine, Northwestern University, Chicago, IL.

Conflicts of interest and sources of funding: Support by the American Heart Association (12GRNT12080032) and the National Institutes of Health (1R21HL113895). The authors report no conflicts of interest.

Correspondence to: Michael Markl, PhD, Department of Radiology, Feinberg School of Medicine, Northwestern University, 737 N Michigan Ave, Suite 1600, Chicago, IL 60611. E-mail: mmarkl@northwestern.edu.



ISSN: 0020-9996/15/0000–0000
DOI: 10.1097/RLI.0000000000000219

motion.[18,22] Further 4D flow MRI pulse sequence parameters were as follows: flip angle, 7 degrees; spatial resolution, 2.5–3.0 × 2.5–3.0 × 3.0–4.0 mm; temporal resolution, 37.6–41.6 milliseconds, imaging acceleration (generalized autocalibrating partially parallel acquisitions technique) with a reduction factor of $R = 2$; total acquisition time of 10 to 20 minutes depending on heart rate and navigator efficiency; and velocity sensitivity of 100 to 150 cm/s. If Gd-contrast administration and contrast-enhanced magnetic resonance angiography (MRA) was part of the standard-of-care imaging protocol, 4D flow data was performed at the end of the MRI examination (ie, 10–15 minutes after Gd injection). In case of contrast agent administration, the flip angle was adjusted to 15 degrees account for different blood T1.

## 4D Flow MRI Data Analysis

Data preprocessing included corrections for Maxwell terms, eddy current-induced phase offsets, and velocity aliasing.[22–24] In addition, 3D PC-MRA data were derived from the 4D flow data and used for creating a 3D segmentation of the LA (Mimics; Materialise).[25–27] As illustrated in Figure 1A, the resulting 3D segmentation mask was used to quantify LA volume and to isolate the velocity data in the LA volume for all atrial voxels and all cardiac time frames. The resulting 4D flow MRI data provide information on 3-directional flow velocities [$v_x(t)$, $v_y(t)$, $v_z(t)$] over the cardiac cycle within the segmented LA volume ($t$ indicates time in the cardiac cycle). For further hemodynamic analysis, absolute atrial velocities

$$v(t) = \sqrt{v_x(t)^2 + v_y(t)^2 + v_z(t)^2}$$

were calculated for each voxel inside the segmented LA and used to derive LA stasis, peak velocity, and TTP maps oriented in sagittal oblique orientation as illustrated in Figure 1B. Mean LA velocity (averaged over all LA voxels and cardiac time frames) was calculated.

### Atrial Stasis Maps

For each voxel inside the segmented LA, the relative amount of flow stasis $r_{stasis}$ (in percent) was calculated by determining the number of cardiac time frames $n_{stasis}$ with velocities below a threshold [$v(t) < v_{stasis\_thresh}$] normalized by the total number of cardiac time frames $N_{Tot}$: $r_{stasis} = n_{stasis}/N_{Tot} \times 100$. Stasis maps were generated by projecting the mean relative stasis on a 2D plane transecting the LA and were color coded for intuitive identification of regions with low versus high stasis (Fig. 1B, left).

### Peak LA Velocity 4D Maximum Intensity Projections

For each voxel inside the segmented LA, the maximum velocity ($v_{max}$) within the cardiac cycle was extracted. The maximum intensity projection (MIP) over all $v_{max}$ was calculated resulting in a 4D (3D + time) MIP of LA peak velocities (Fig. 1B, mid).

### TTP Maps

To quantify regional differences in timing of high LA flow velocities with respect to the beginning of the cardiac cycle (as defined by the R-wave), the TTP velocity for each voxel inside the segmented LA was determined. Time-to-peak maps were generated by projecting mean TTP on a 2D plane (Fig. 1B, right).

All maps were overlaid onto the underlying anatomic 4D flow MRI data for improved anatomic orientation (see Fig. 1B). To evaluate interobserver variability, a second independent observer, blinded to the other reader's results, reanalyzed the LA 4D flow data by performing a second 3D segmentation of the LA in a subgroup of 29 subjects.

### Quantification of Global and Regional Metrics of LA Flow Dynamics

Global stasis and TTP for the entire LA were calculated by averaging over all LA voxels. The overall peak LA velocity was calculated as the average over the top $v_{peakvel\_thresh}$% of all LA velocities (3D and time over the cardiac cycle). As the pathophysiology of thromboembolism in AF is based upon formation of mural thrombi, regional analysis focused on the region adjacent to the LA wall. As illustrated in Figure 1B, regional LA flow analysis was performed on all 3 LA maps (stasis, peak velocity, TTP) by dividing the LA in 2 regions: the LA center region and the region adjacent to the LA wall. In all subjects, the LA center region was automatically generated without user interaction by eroding the segmented LA area by 2 voxels inward from the outer LA boundaries. Subsequently, the region adjacent to the LA wall was calculated by subtracting the LA center region from the original LA segmentation. Average peak velocity, stasis, and TTP were calculated in both regions for all subjects.

## Statistics Sensitivity Analysis: Identification of LA Stasis and LA Peak Velocity Thresholds

All data were analyzed using a range of different velocity thresholds ($v_{stasis\_thresh}$ = 0.02-0.2 m/s in 0.02 m/s steps and $v_{peakvel\_thresh}$ = 1%–10% in 1% steps) to assess their influence on LA flow parameters

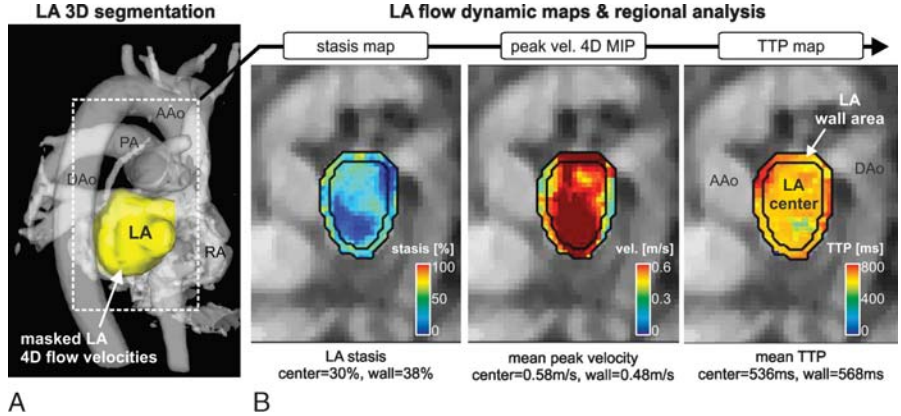


**FIGURE 1.** Four-dimensional flow MRI data analysis in a 62-year-old male patient with a history of AF (AF-sinus, subject 35) including A, 3D segmentation of the LA based on the 3D PC-MRA data (gray-shaded isosurface) and masking of velocities inside the segmented LA. B, Calculation of LA stasis maps for a velocity threshold of 0.1 m/s (left), peak velocity MIPs (mid), and TTP velocity maps. Atrial areas for the analysis regional velocities and stasis in the LA center and adjacent to the LA wall are delineated by black lines. The mean for all 3 metrics of regional LA flow dynamics are listed below each map. AAo indicates ascending aorta; DAo, descending aorta; PA, pulmonary artery.

**TABLE 1.** Demographics of Study Cohorts

| | n | Age, y | Sex, Male/Female | LVEF, % | LA Volume, mL | Heart Rate, beats per minute |
|---|---|---|---|---|---|---|
| Young controls | 10 | 24 ± 2 | 6/4 | 62 ± 4 | 25 ± 5 | 63 ± 8 |
| Age controls | 20 | 59 ± 7 | 13/7 | 62 ± 1 | 37 ± 12* | 68 ± 11 |
| AF-sinus patients | 42 | 62 ± 11 | 29/13 | 58 ± 8 | 64 ± 29† | 68 ± 15 |
| AF-afib patients | 39 | 66 ± 11 | 27/11 | 54 ± 10‡ | 93 ± 58‡§ | 78 ± 15§ |

Differences between groups were considered significant for $P < 0.0125$ (Bonferroni correction for multiple comparisons).

*Significant difference old versus young controls.

†Significant difference old controls versus AF-sinus.

‡Significant difference old controls versus AF-afib.

§Significant difference AF-sinus versus AF-afib.

LVEF indicates left ventricular ejection fraction; LA, left atrium; AF-sinus, atrial fibrillation and in sinus rhythm; AF-afib, persistent atrial fibrillation.

and differences in LA flow dynamics between groups (young and older controls, AF-sinus, AF-afib). For each group, a Shapiro-Wilk test was used to determine if parameters were normally distributed. To compare parameters among the 4 groups, 1-way analysis of variance (Gaussian distribution) or Kruskal-Wallis (non-Gaussian distribution) was used. If these tests determined that a parameter was significantly different among groups ($P < 0.05$), multiple comparisons between groups were performed using independent sample *t* tests (Gaussian distribution) or Mann-Whitney *U* tests (non-Gaussian distribution). Bonferroni correction was used to adjust for multiple comparisons, and differences were considered significant for $P < 0.0125$.

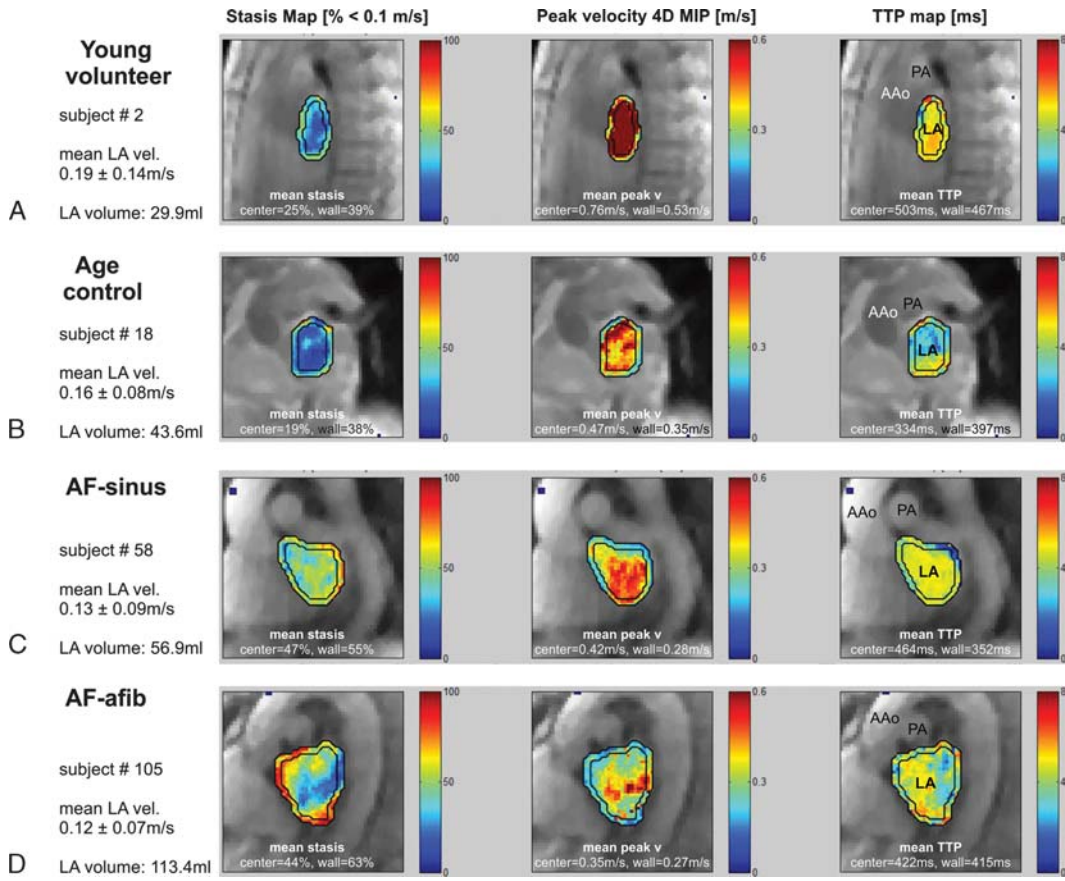


**FIGURE 2.** Maps of LA flow parameters superimposed on the underlying anatomic 4D flow MRI data in oblique sagittal orientation. The individual images show stasis maps for a velocity threshold of 0.1 m/s (left column), peak velocity MIPs (4D, mid column), and TTP velocity maps (right column) in 4 subjects representing each of the subgroups (A–D). Color coding illustrates regions in the LA with high (red) and low (blue) stasis, peak velocity, and TTP. Areas for the analysis of regional flow dynamics (LA center and LA wall) are delineated, and the resulting regional LA stasis, peak velocities, and TTP are listed below each map. AAo indicates ascending aorta; PA, pulmonary artery.

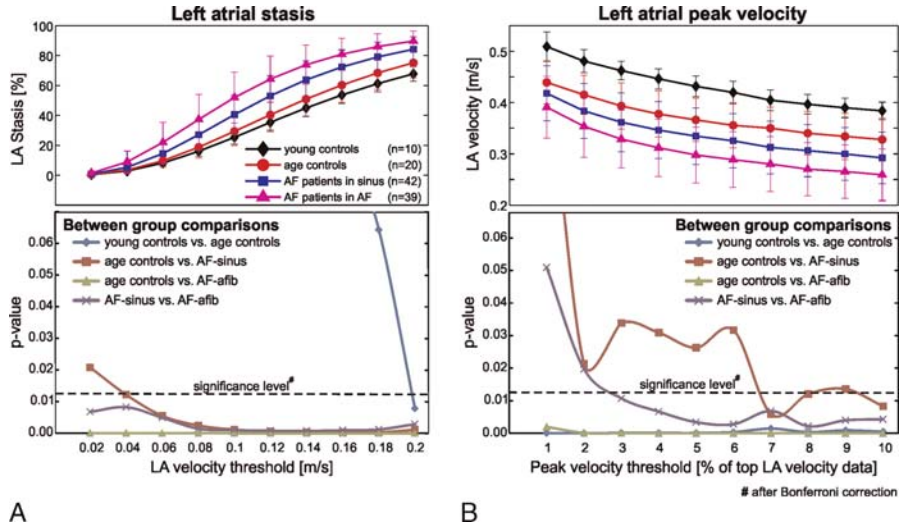


**FIGURE 3.** Sensitivity analysis for the identification of LA stasis and LA peak velocity thresholds. A, LA stasis (top) as a function of the LA velocity threshold (% LA velocities < LA velocity threshold, $v_{stasis\_thresh}$) for all 4 groups (young volunteers, age-appropriate controls, AF-sinus, AF-afib). Corresponding *P* values for pairwise comparisons of LA stasis between groups are shown below. B, Peak LA velocities (top) for different thresholds (% of top LA velocities, $v_{peakvel\_thresh}$) and *P* values for between group comparisons (bottom). The individual data points represent averaged over all subjects in each group. Error bars indicate interindividual standard deviations of LA flow metrics. Figure 3 can be viewed online in color at www.investigativeradiology.com.

## Statistics Relationships Between LA Flow Metrics and Patient Characteristics

To identify relationships between metrics of LA flow (mean velocity, peak velocity, stasis, TTP) with demographic and geometric parameters (age, heart rate, LVEF, LA volume), Pearson correlation coefficients *r* were calculated to identify variables for subsequent multiple linear regression analysis ($r \geq 0.25$). The aim was to quantify the relationship between impaired LA flow metrics (dependent parameters) and demographics and geometric parameters as independent predictors. The overall quality of the model was quantified using the adjusted $R^2$ ($R^2_{Adj}$). The relative contributions of the demographic and geometric parameters were determined from the standardized regression coefficients β. A correlation was considered significant for $P < 0.05$.

# RESULTS

## Patient Characteristics

Patient demographics are summarized in Table 1. The AF population was predominantly male, and AF cohorts had significantly increased LA volumes compared with the age-appropriate controls. In addition, LA volume (64 ± 29 mL vs 93 ± 58 mL, $P = 0.005$) and heart rate (68 ± 15 beats per minute vs 78 ± 15 beats per minute, $P = 0.003$) were significantly higher in AF-afib patients compared with AF-sinus subjects.

## Left Atrial Stasis, Peak Velocity, and TTP Maps

Examples of LA flow parameter maps (stasis, peak velocity, TTP) for 4 representative subjects of each cohort are shown in Figure 2. Four-dimensional flow MRI in a young HV (Fig. 2A) revealed high-peak velocities throughout the LA and lowest stasis compared with the 3 subjects from other groups. In all subjects, LA stasis based on a velocity threshold of 0.1 m/s showed an inhomogeneous pattern and was higher adjacent to the LA wall compared with the central region of the LA, which was confirmed by regional LA stasis quantification (see mean stasis for LA center and LA wall below individual maps). The age-appropriate control subject (Fig. 2B) showed similar regional LA stasis patterns but considerably reduced LA peak velocities in both LA regions (average reduction by 38% and 34%, respectively). Atrial fibrillation patients (Fig. 2, C and D) showed higher stasis throughout the LA (particularly adjacent to the LA wall) and lower and more

**TABLE 2.** Descriptive Statistics for Global Metrics of LA Flow Dynamics

| | n | Mean LA Velocity, m/s | Stasis <0.1 m/s, % | Peak Velocity 5%, m/s | TTP, ms |
|---|---|---|---|---|---|
| Young controls | 10 | 0.18 ± 0.02 | 25 ± 5 | 0.43 ± 0.02 | 480 ± 50 |
| Age controls | 20 | 0.16 ± 0.02* | 29 ± 10 | 0.37 ± 0.04* | 410 ± 60* |
| AF-sinus patients | 42 | 0.13 ± 0.02† | 41 ± 13† | 0.33 ± 0.05 | 420 ± 90 |
| AF-afib patients | 39 | 0.11 ± 0.03‡§ | 52 ± 17‡§ | 0.30 ± 0.05‡§ | 400 ± 90 |

Differences between groups were considered significant for $P < 0.0125$ (Bonferroni correction for multiple comparisons).

*Significant difference age-appropriate versus young controls.

†Significant difference age-appropriate controls versus AF-sinus.

‡Significant difference age-appropriate controls versus AF-afib.

§Significant difference AF-sinus versus AF-afib.

LA indicates left atrium; TTP, time-to-peak; AF-sinus, atrial fibrillation and in sinus rhythm; AF-afib, persistent atrial fibrillation.

**TABLE 3.** Summary of the Results of Regional LA Flow Analysis Based on Stasis, Peak Velocity, and TTP Maps

| | | Regional Stasis <0.1 m/s, % | | Regional Mean Peak Velocity, m/s | | Regional Mean TTP, ms | |
|---|---|---|---|---|---|---|---|
| | n | Center | Wall | Center | Wall | Center | Wall |
| Young controls | 10 | 23 ± 5 | 32 ± 4 | 0.59 ± 0.09 | 0.54 ± 0.09 | 482 ± 53 | 463 ± 52 |
| Age controls | 20 | 28 ± 10 | 36 ± 8 | 0.44 ± 0.10* | 0.40 ± 0.11* | 411 ± 63* | 396 ± 59* |
| AF-sinus patients | 42 | 39 ± 13† | 46 ± 14† | 0.41 ± 0.09 | 0.39 ± 0.11 | 425 ± 86 | 386 ± 88 |
| AF-afib patients | 39 | 51 ± 17‡§ | 56 ± 16‡§ | 0.36 ± 0.09‡ | 0.31 ± 0.10‡§ | 408 ± 93 | 381 ± 88 |

Differences between groups were considered significant for $P < 0.0125$ (Bonferroni correction for multiple comparisons).

*Significant difference age-appropriate versus young controls.

†Significant difference age-appropriate controls versus AF-sinus.

‡Significant difference age-appropriate controls versus AF-afib.

§Significant difference AF-sinus versus AF-afib.

LA indicates left atrium; TTP, time-to-peak; AF-sinus, atrial fibrillation and in sinus rhythm; AF-afib, persistent atrial fibrillation.

heterogeneous distribution of LA peak velocities (specifically for AF-afib, Fig. 2D) compared with control subjects. Time-to-peak did not show consistent differences among groups.

## Sensitivity Analysis: Identification of LA Stasis and LA Peak Velocity Thresholds

Figure 3 shows the results of the analysis of different thresholds for global LA stasis and peak velocity quantification. Except for young versus age-appropriate controls, LA stasis (Fig. 3A) was significantly different between each of the groups (age matched controls, AF-sinus, AF-afib) for $v_{stasis\_thresh}$ 0.04 m/s or greater. Left atrial stasis could robustly differentiate between these groups for a wide range of velocity thresholds ($P \leq 0.001$ for $v_{stasis\_thresh}$ ranging from 0.10 to 0.18 m/s). Findings for LA peak velocities are shown in Figure 3B. Significant differences ($P < 0.0125$) between each of the groups were found for a wide range of thresholds $v_{peakvel\_thresh}$ 3% or greater (except for AF-sinus vs age-appropriate controls). For further analysis of global LA stasis and

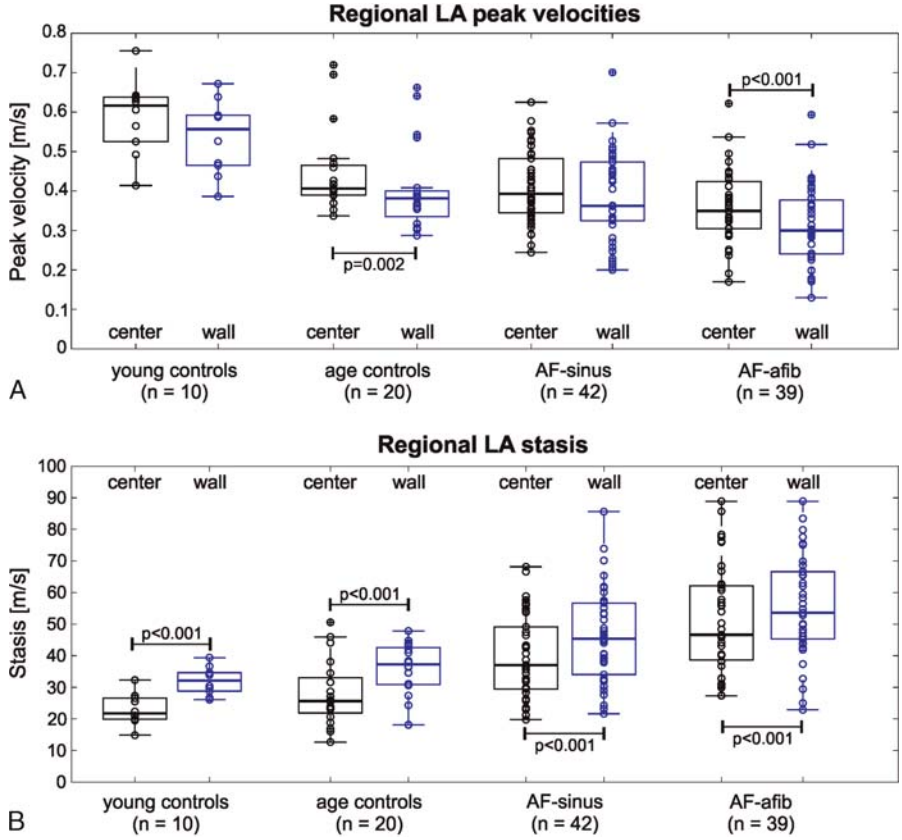


**FIGURE 4.** Groupwise comparisons of regional LA peak velocities (A) and LA stasis (B). Flow stasis adjacent to the LA wall was significantly elevated compared with the LA center for all subject groups. The individual box plots illustrate the median (central mark) and the 25th and 75th percentiles (edges), the whiskers extend to the most extreme data points not considered outliers, and outliers are plotted individually as "+". Figure 4 can be viewed online in color at www.investigativeradiology.com.

**TABLE 4.** Multiple Linear Regressions of Global LA Flow Metrics with Heart Rate, Age, and LA Volume as Independent Predictors in n = 111 Subjects

| | Model Quality | | Age | | Heart Rate | | LA Volume | |
|---|---|---|---|---|---|---|---|---|
| **LA Flow Metric** | $R^2_{Adj}$ | ***P*** | β | ***P*** | β | ***P*** | β | ***P*** |
| Mean LA velocity | **0.50** | **<0.001** | **−0.42** | **<0.001** | −0.09 | NS | **−0.39** | **<0.001** |
| Stasis < 0.1 m/s | **0.45** | **<0.001** | **0.27** | **0.001** | 0.09 | NS | **0.50** | **<0.001** |
| Peak velocity, 5% | **0.46** | **<0.001** | **−0.50** | **<0.001** | −0.10 | NS | **−0.26** | **0.002** |

The significance of the model was assessed using the overall *P* value, and the percent of variance explained using the adjusted $R^2$ ($R^2_{Adj}$). The relative contributions of the geometric parameters are given by the standardized regression coefficients β. Significant correlations ($P < 0.05$) are indicated by bold numbers.

LA indicates left atrium; NS, not significant.

peak velocity, $v_{stasis\_thresh}$ of 0.1 m/s and $v_{peakvel\_thresh}$ of 5% were chosen, respectively.

## Group Wise Comparisons of Global Metrics of LA Flow

For all analyzed global LA flow metrics (LA mean velocity, stasis, peak velocity, TTP), significant differences across all 4 groups were found (analysis of variance or Kruskal-Wallis, $P < 0.0001$). Subsequent multiple comparisons between groups (Table 2) demonstrated significant differences ($P < 0.0125$) for LA mean velocity, stasis, and peak velocity except for peak LA velocities between age matched controls versus AF-sinus patients ($P = 0.026$).

## Regional LA Velocities and Stasis

The results of the regional analysis of LA flow dynamics (LA center vs regions adjacent to the LA wall) are summarized in Table 3 and Figure 4. Multiple comparisons (Table 3) demonstrated significantly increased stasis in all regions for both AF patient groups (AF-sinus, AF-afib) compared with age-appropriate controls (29%–84% difference, $P < 0.006$) and for AF-afib compared with AF-sinus patients (22%–30% difference, $P < 0.004$). As illustrated in Figure 4, flow stasis adjacent to the LA wall was significantly elevated ($P < 0.001$) compared with the LA center for all 4 subject groups. Regional peak velocities were generally lower for AF patients compared with controls and reduced adjacent to the LA wall compared with the LA center, which was, however, only significant for age-appropriate controls and AF-afib patients (Fig. 4).

## Relationships Between LA Flow Metrics and Patient Characteristics

As summarized in Table 4, multiple linear regressions revealed significant relationships ($P \leq 0.002$) between reduced global mean and peak LA velocities and age and LA volume but not with heart rate. Similarly, the extent of the LA exposed to flow stasis demonstrated significant relationships with age and LA volume but not with heart rate.

## Interobserver Variability

Bland-Altman plots demonstrated good interobserver agreement for measurements of mean LA velocity, peak LA velocity, and LA stasis (Fig. 5). Observer variability resulted in average interobserver differences of 6.0% for mean velocity, 10.2% for global LA stasis, and 7.9% for global LA peak velocity.

# DISCUSSION

The findings of this study demonstrate the potential of 4D flow MRI for the comprehensive assessment of global and regional LA flow dynamics. The analysis to identify velocity thresholds for LA stasis and LA peak velocity that could differentiate among all 4 patient and controls groups revealed a wide range of significant thresholds, supporting the robustness of the technique. In addition, regional stasis was consistently elevated adjacent to the LA wall compared with the LA center in all study groups and was significantly elevated for AF patients compared with controls. These results indicate the potential of atrial 4D flow MRI to detect differences in global LA stasis and LA peak velocity related to rhythm (sinus vs AF) in patients with AF and regional differences in stasis related to LA flow physiology (reduced flow and elevated stasis adjacent to the LA wall). Moreover, significant associations of impaired LA flow (reduced mean and peak velocity and increased stasis) with LA volume point to a physiologic structure-function relationship between altered LA geometry and hemodynamics.

It was initially hypothesized that LA TTP velocity might be a useful measure to detect disorganized flow in patients with AF (inconsistent timing of the occurrence of peak velocity across the LA). However, neither global nor regional LA TTP velocity was sensitive to detect differences in LA flow patterns. Based on these findings, we speculate that reduction of LA peak velocities and in particular increase in regional LA stasis are more sensitive markers of altered LA flow compared with the simple measure of the timing of LA flow (TTP) used in this study.

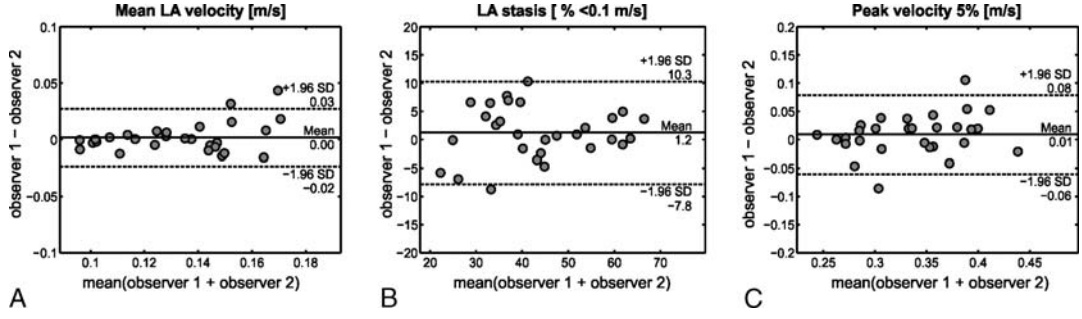


**FIGURE 5.** Bland-Altman analysis of interobserver variability for the quantification of mean LA velocity, peak LA velocity ($v_{peakvel\_thresh}$ = 5%), and LA stasis ($v_{stasis\_thresh}$ = 0.1 m/s) in a subgroup of n = 29 subjects.

Four-dimensional flow MRI has previously been applied for the in vivo study of LA blood flow in a number of studies.[12,13,18–20,28,29] The technique is noninvasive and provides time-resolved 3D LA blood flow velocities with full volumetric coverage of the LA. Previous studies were either based on small cohorts to evaluate normal and pathological flow physiology, such as the presence and extent of vortex flow in the heart and atria,[12,19,20] to study the asymmetric redirection of flow through the entire heart,[13] or to assess the impact of atrial-septal defects and shunt flows.[29] A recent study by Suwa et al[28] investigated the relationship between LA vortex flow, heart diseases, and LA volume. Similar to findings in our study, the authors found associations between changes in LA flow and volume.

Previous studies, however, were based on 3D blood flow visualization (using vector fields, time resolved path lines, or streamlines) and qualitative evaluation of flow features (semiquantitative schemes to grade atrial vortex flow) or regional flow quantification based on 2D analysis planes. In contrast, our study utilized the complete 3-directional velocity information in the entire LA and over the cardiac cycle to visualize LA flow using maps that quantify metrics reflecting 4D (3D + time) flow parameters. Four-dimensional flow-derived stasis maps and peak velocity 4D MIPs are a new concept offering intuitive visualization of otherwise complex 4D flow MRI data. In addition, 3D segmentation of the LA enabled an automated regional analysis of LA flow dynamics by systematic inward erosion of the map area and calculation of velocities and stasis in the LA center and a 2-voxel region adjacent to the LA wall. Such patient-specific maps in conjunction with regional quantification could potentially identify regions with elevated stasis, which are thought to promote thrombus formation and thus risk for stroke. Such regional information could be useful when considering therapies for stroke prevention in AF that address only localized areas, such as LA appendage (LAA) occlusion devices. Future studies should include a more detailed assessment of regional differences in LA flow patterns (eg, LA vs LAA velocities and stasis) to further elucidate the role of regional variability of LA flow and stasis in LA thrombus formation. These studies can also help to better define the diagnostic value of reducing the LA flow information into a single parameter (eg, global LA stasis or global LA peak velocity) versus maintaining a 2D stasis map for additional visual interpretation.

A number of Doppler echocardiography studies have previously investigated LA blood flow velocities. In a TEE study with 721 AF patients, Goldman et al[3] reported reduced peak LAA velocity in patients with AF compared with those in sinus rhythm during TEE (33 vs 61 cm/s, $P < 0.001$). The selection of velocity thresholds for the sensitivity analysis in our study was based on results from this TEE study which found that peak antegrade LAA (emptying) flow velocity less than 0.2 m/s was associated with increased risk for atrial thrombus formation and embolic stroke.[3] Another study by Handke et al[4] also found significant differences in LA peak velocities among patients with sinus rhythm (71 ± 16 cm/s) and with cardiac arrhythmia during TEE (46 ± 13 cm/s). In agreement with these studies, our patient cohort exhibited differences in LA flow velocities between AF patients in sinus rhythm and with cardiac arrhythmia during 4D flow MRI. However, LA peak velocities in our study cohort were lower (0.30-0.43 m/s) compared with findings in previous TEE studies. This underestimation of peak velocities may be attributed to the lower spatial and temporal resolution of 4D flow MRI compared with TEE. Nevertheless, both 4D flow-derived LA peak velocity and LA stasis could detect significant differences between AF patient and control groups.

## Study Limitations

The present study evaluated LA velocity maps measured with 4D flow MRI in patients with AF (paroxysmal vs persistent), HVs, and age-matched controls. The main limitation of this study is related to it cross-sectional design. Clinical risk scores or data on other factors that may affect LA velocity maps such as mitral regurgitation or stenosis were not available. In addition, information on mitral valve function and diastolic dysfunction was not available for the AF patients in our study cohort. Furthermore, no follow-up in terms of intra-LA thrombus formation was performed, which was beyond the scope of this feasibility study. Additional longitudinal studies are thus needed to further test the diagnostic value of 4D flow-derived LA for metrics for risk stratification of AF patients for future thromboembolic events.

Our study demonstrated significant associations between LA volume and LA velocities and stasis. However, a more detailed analysis of LA and LAA geometry and shape and its association with LA flow parameters was not performed. Our study design was based on an analysis workflow targeting a cardiac region (the LA) that could reliably be segmented and analyzed based on the 4D flow MRI contrast and spatial resolution, as was demonstrated by the very good observer variability we found in our study. In this context, additional studies need to be conducted to investigate if the contrast and resolution of 4D flow data will be sufficient to identify the LAA boundaries for a reliable assessment of LAA size, anatomy, and flow dynamics. Future studies should thus systematically evaluate differences in LA versus LAA flow dynamics and test the feasibility, reproducibility, and observer variability of the quantification LAA size, anatomy, and flow dynamics based on 4D flow MRI.

A further limitation is related to the selection of the velocity sensitivity of the 4D flow MRI acquisition, which was in the range of 100 to 150 cm/s (ie, larger than typical atrial flow velocities) to avoid velocity aliasing. However, no velocity scout scan was performed to better tailor the velocity sensitivity to the atrial velocities in the individual patient to optimize the velocity-to-noise ratio of the LA 4D flow data. Another drawback is the long scan times on the order of 10 to 20 minutes needed to collect atrial 4D flow MRI data. As a result, beat-to-beat flow variations in AF patients with cardiac arrhythmia cannot be captured by this technique. Nevertheless, the blood flow measurements made with 4D flow MRI represent the average flow patterns over the entire length of the acquisition that are consistent over several cardiac cycles. This underlying assumption was confirmed by a recently performed validation study.[21] Based on real time in vivo TEE data in 5 AF patients with known arrhythmia, a simulation study systematically investigated the impact of beat-to-beat variations on ECG-gated multibeat flow imaging with MRI. Results demonstrated that ECG-gated multibeat flow MRI in patients with cardiac arrhythmia could reproduce persistent average LA and left ventricular mean velocities within 7.0% to 7.4% compared with TEE. These findings demonstrate that 4D flow MRI can reliably assess persistent atrial flow and stasis patterns that are consistently present over multiple heart beats. Because LA thrombus, the main source of embolic stoke in AF patients, will form over longer periods, we speculate that these persistent flow features representing long-term patterns over multiple RR intervals (eg, elevated LA stasis) could be important physiologic markers for thrombus formation and this thromboembolic risk.

## CONCLUSIONS

The findings of this study indicate that atrial 4D flow MRI and derived in vivo peak velocity and stasis maps are robust tools for the detection changes in global and regional flow dynamics in the LA associated with AF, patient age, and LA volume. Additional longitudinal studies are warranted to test the diagnostic value of LA flow metrics as potential risk factors for thromboembolic events.

## REFERENCES

1. Chugh SS, Havmoeller R, Narayanan K, et al. Worldwide epidemiology of atrial fibrillation: a global burden of disease 2010 study. *Circulation*. 2013;129:837–47.
2. Fuster V, Rydén LE, Cannom DS, et al. 2011 ACCF/AHA/HRS focused updates incorporated into the ACC/AHA/ESC 2006 guidelines for the management of patients with atrial fibrillation: a report of the American College of Cardiology

Foundation/American Heart Association task force on practice guidelines. *Circulation*. 2011;123:e269–e367.

3. Goldman ME, Pearce LA, Hart RG, et al. Pathophysiologic correlates of thromboembolism in nonvalvular atrial fibrillation: I. Reduced flow velocity in the left atrial appendage (the stroke prevention in atrial fibrillation [SPAF-III] study). *J Am Soc Echocardiogr*. 1999;12:1080–1087.
4. Handke M, Harloff A, Hetzel A, et al. Left atrial appendage flow velocity as a quantitative surrogate parameter for thromboembolic risk: determinants and relationship to spontaneous echocontrast and thrombus formation—a transesophageal echocardiographic study in 500 patients with cerebral ischemia. *J Am Soc Echocardiogr*. 2005;18:1366–1372.
5. Pollick C, Taylor D. Assessment of left atrial appendage function by transesophageal echocardiography. Implications for the development of thrombus. *Circulation*. 1991;84:223–231.
6. Transesophageal echocardiographic correlates of thromboembolism in high-risk patients with nonvalvular atrial fibrillation. The Stroke Prevention in Atrial Fibrillation Investigators Committee on Echocardiography. *Ann Intern Med*. 1998;128:639–647.
7. Asinger RW, Koehler J, Pearce LA, et al. Pathophysiologic correlates of thromboembolism in nonvalvular atrial fibrillation: II. Dense spontaneous echocardiographic contrast (the stroke prevention in atrial fibrillation [SPAF-III] study). *J Am Soc Echocardiogr*. 1999;12:1088–1096.
8. Predictors of thromboembolism in atrial fibrillation: II. Echocardiographic features of patients at risk. The stroke prevention in atrial fibrillation investigators. *Ann Intern Med*. 1992;116:6–12.
9. Echocardiographic predictors of stroke in patients with atrial fibrillation: a prospective study of 1066 patients from 3 clinical trials. *Arch Intern Med*. 1998;158:1316–1320.
10. Di Biase L, Santangeli P, Anselmino M, et al. Does the left atrial appendage morphology correlate with the risk of stroke in patients with atrial fibrillation? Results from a multicenter study. *J Am Coll Cardiol*. 2012;60:531–538.
11. Markl M, Kilner PJ, Ebbers T. Comprehensive 4D velocity mapping of the heart and great vessels by cardiovascular magnetic resonance. *J Cardiovasc Magn Reson*. 2011;13:7.
12. Ebbers T, Wigström L, Bolger AF, et al. Noninvasive measurement of time-varying three-dimensional relative pressure fields within the human heart. *J Biomech Eng*. 2002;124:288–293.
13. Kilner PJ, Yang GZ, Wilkes AJ, et al. Asymmetric redirection of flow through the heart. *Nature*. 2000;404:759–761.
14. François CJ, Srinivasan S, Schiebler ML, et al. 4D cardiovascular magnetic resonance velocity mapping of alterations of right heart flow patterns and main pulmonary artery hemodynamics in tetralogy of Fallot. *J Cardiovasc Magn Reson*. 2012;14:16.
15. Eriksson J, Carlhäll CJ, Dyverfeldt P, et al. Semi-automatic quantification of 4D left ventricular blood flow. *J Cardiovasc Magn Reson*. 2010;12:9.
16. Roes SD, Hammer S, van der Geest RJ, et al. Flow assessment through four heart valves simultaneously using 3-dimensional 3-directional velocity-encoded magnetic resonance imaging with retrospective valve tracking in healthy volunteers and patients with valvular regurgitation. *Invest Radiol*. 2009;44:669–675.
17. Uribe S, Beerbaum P, Sørensen TS, et al. Four-dimensional (4D) flow of the whole heart and great vessels using real-time respiratory self-gating. *Magn Reson Med*. 2009;62:984–992.
18. Fluckiger JU, Goldberger JJ, Lee DC, et al. Left atrial flow velocity distribution and flow coherence using four-dimensional flow MRI: a pilot study investigating the impact of age and pre- and postintervention atrial fibrillation on atrial hemodynamics. *J Magn Reson Imaging*. 2013;38:580–587.
19. Föll D, Taeger S, Bode C, et al. Age, gender, blood pressure, and ventricular geometry influence normal 3D blood flow characteristics in the left heart. *Eur Heart J Cardiovasc Imaging*. 2013;14:366–373.
20. Fyrenius A, Wigström L, Ebbers T, et al. Three dimensional flow in the human left atrium. *Heart*. 2001;86:448–455.
21. Markl M, Fluckiger JU, Lee DC, et al. Velocity quantification by electrocardiography-gatedphase contrast magnetic resonance imaging in patients with cardiac arrhythmia: a simulation study based on real time transesophageal echocardiography data in atrial fibrillation. *J Comput Assist Tomogr*. 2015;39:422–427.
22. Markl M, Harloff A, Bley TA, et al. Time-resolved 3D MR velocity mapping at 3T: improved navigator-gated assessment of vascular anatomy and blood flow. *J Magn Reson Imaging*. 2007;25:824–831.
23. Bock J, Kreher B, Hennig J, et al. Optimized pre-processing of time-resolved 2D and 3D phase contrast MRI data. *Proceedings of the 15th Annual Meeting of ISMRM, Berlin, Germany*. 2007:3138.
24. Walker PG, Cranney GB, Scheidegger MB, et al. Semiautomated method for noise reduction and background phase error correction in MR phase velocity data. *J Magn Reson Imaging*. 1993;3:521–530.
25. Bock J, Frydrychowicz A, Stalder AF, et al. 4D phase contrast MRI at 3 T: effect of standard and blood-pool contrast agents on SNR, PC-MRA, and blood flow visualization. *Magn Reson Med*. 2010;63:330–338.
26. Dumoulin CL. Phase contrast MR angiography techniques. *Magn Reson Imaging Clin N Am*. 1995;3:399–411.
27. Frydrychowicz A, François CJ, Turski PA. Four-dimensional phase contrast magnetic resonance angiography: potential clinical applications. *Eur J Radiol*. 2011;80:24–35.
28. Suwa K, Saitoh T, Takehara Y, et al. Characteristics of intra-left atrial flow dynamics and factors affecting formation of the vortex flow—analysis with phase-resolved 3-dimensional cine phase contrast magnetic resonance imaging. *Circ J*. 2015;79:144–52.
29. Valverde I, Simpson J, Schaeffter T, et al. 4D phase-contrast flow cardiovascular magnetic resonance: comprehensive quantification and visualization of flow dynamics in atrial septal defect and partial anomalous pulmonary venous return. *Pediatr Cardiol*. 2010;31:1244–1248.